International Journal of Adhesion & Adhesives 36 (2012) 77–85

Contents lists available at SciVerse ScienceDirect

International Journal of Adhesion & Adhesives

journal homepage: www.elsevier.com/locate/ijadhadh

The effect of adhesive thickness on tensile and shear strength of polyimide adhesive

Kimiyoshi Naito [a,*], Mutsumi Onta [b], Yasuo Kogo [b]

[a] National Institute for Materials Science, Hybrid Materials Unit, Composite Materials Group, 1-2-1 Sengen, Tsukuba, Ibaraki 305 0047, Japan
[b] Tokyo University of Science, Faculty of Industrial Science and Technology, 2641 Yamazaki, Noda, Chiba 278 8510, Japan

ARTICLE INFO

Article history:
Accepted 1 March 2012
Available online 22 March 2012

Keywords:
High temperature adhesives
Polyimide
Aluminum and alloys
Butt joints
Lap-shear
Stress analysis
Stress distribution
Fracture

ABSTRACT

The effect of adhesive thickness on tensile and shear strength of a polyimide adhesive has been investigated. Tensile and shear tests were carried out using butt and single lap joints. Commercially available polyimide (Skybond 703) was used as adhesive and aluminum alloy (5052-H34) was used as adherends. The tensile strength of the butt joints decreased with increasing adhesive thickness. In contrast, adhesive thickness did not seem to affect the shear strength of single lap joints. The fabricated joints using the polyimide adhesive failed in an interfacial manner regardless of adhesive thickness. The linear elastic stress analysis using a finite element method (FEM) indicates that the normal stress concentrated at the interface between the adherend and the adhesive. The FEM analysis considering the interfacial stress well explains the effect of adhesive thickness on the joint strength.

1. Introduction

Aluminum, titanium alloys and fiber reinforced polymer-based composites (FRP) are widely used as the lightweight structural materials in numerous industrial applications since they have superior mechanical properties [1–3]. Adhesive bonding is formerly applied for such lightweight structural materials [4,5]. Epoxies are one of the successful adhesives and are widely used as high-performance structural adhesives, especially in automotive and aircraft manufacture because of their ability to cure without producing volatile by-products and their low shrinkage upon curing [6,7]. However, usable temperature range of epoxies is less than 200 °C [8–11]. In a variety of industrial applications, adhesives are required to have a high temperature range. Polyimides are an important class of high temperature polymers for use as structural adhesives because of their intrinsic thermal, thermo-oxidative, and chemical stability coupled with high mechanical properties [8,12,13]. However, fabricating polyimides is difficult since they produce volatiles by chemical reaction and from residual solvent during curing [8,12–14]. The aromatic polyimides are insoluble and infusible, a polyimide precursor consisting of polyamic acid in a high boiling polar solvent such as n-methylpyrrolidone. As polyamic acid convert to polyimide through curing after bonding, volatilization of all solvents and by-products results in voids in the polyimide adhesive. Some studies [15–17] suggest that these voids are created by evaporation of volatiles and air entrapment. Voids occur easily in an adhesive bonded joint compared with a typical polymer-based adhesive with no solvent and no by-products, e.g., an epoxy adhesive. High hydrostatic pressure during autoclaving [15,18,19] is effective to reduce the void content in the polyimides and the mechanical properties of polyimide adhesives also depend on processing conditions. Although remarkable efforts have been paid to polyimides, the research on polyimide adhesives is still limited.

The traditional evaluation of adhesive joints by strength measurements was utilized in the study. The adhesive strength was determined by utilizing the butt [20–22] and the single-lap shear test [23–27]. The butt and single-lap joint configuration is widely used in the aerospace, automotive, wood and plastic industries [24,25,28,29]. Butt and single-lap joint specimens are economical, practical and easy to make. It is well confirmed that the strength of adhesive bonded joints affects the adhesive thickness. The effect of bond thickness on adhesive performance for various other joints has been reported by some investigators [30–35]. The experiments are also carried out to validate and compare the theoretical predictions of the adhesion strength of adhesive bonds at different adhesive thickness. More meaningful quantitative characterization is very desirable for evaluating the effect of adhesive thickness on the adhesive strength in adhesive-bonded joints.

The objectives of the present work are to fabricate the adhesive bonded joints using high temperature polyimide adhesive and to show the tensile and shear mechanical properties of a polyimide adhesive under static loading. Especially, the attention of this paper

* Corresponding author. Tel.: +81 29 859 2803; fax: +81 29 859 2401.
E-mail address: naito.Kimiyoshi@nims.go.jp (K. Naito).

0143-7496/$ - see front matter © 2012 Elsevier Ltd. All rights reserved.
http://dx.doi.org/10.1016/j.ijadhadh.2012.03.007

is focused to obtain the effect of adhesive thickness on the tensile and shear strength for these joints of polyimide adhesive.

2. Experimental

2.1. Specimens and materials

Tensile and tensile shear tests were carried out using butt and single lap joint specimens. Fig. 1 shows the shapes and dimensions of the specimens used in this study.

Commercially available solution of aromatic polyimide precursor in ethanol and N-methylpyrrolidone (NMP) (Skybond 703, 3,3′,4,4′-benzophenone tetracarboxylic dianhydraide (BTDA)/3,3′-methlylene-dianiline (MDA), Industrial Summit Technology Co.) was used as a polyimide adhesive. An aluminum alloy (5052-H34) was used for the adherends. Fig. 2 shows the typical tensile stress–strain curves for the bulk polyimide [36] and the aluminum alloy [37] from dog bone type specimens.

2.2. Specimen preparation

Fig. 3 shows the specimen preparation procedure.

Two pieces of adherends were prepared and the surfaces of the adherends were treated with sandblast. The treated adherends were cleaned and degreased by acetone and dried at room temperature under the laboratory environment (at 23 ± 3 °C and 50 ± 5% relative humidity) before bonding. The adherends were degassed at 90 ± 10 °C for 30 min in a vacuum oven for removing bubble after polyimide precursor solution had been spread. The adhesive thickness of butt and single lap joints were controlled by the amount of precursor solution.[1] They were kept at 90 ± 10 °C for 12 h without vacuum for removing solvent. The contents were set to the each tool (fixture and spacer) and pressed at up to 0.7 MPa with vacuum bag (-0.101 MPa) in an autoclave (ACA Series, Ashida Mfg. Co., Ltd.) and heated up gradually to 343 °C. Fig. 4 shows the profile of temperature, vacuum pressure and pressure in the autoclave reactor as a function of time. To remove the residual solvent and the bond between the layers caused by the softening of polyimides, they were heated to 150 and 200 °C, respectively. To fully cure the polyimides for imidization, the materials were heated at 250 and 343 °C, respectively.[2]

Fabricating polyimide adhesive joints is difficult because polyimides produce volatiles during chemical reactions; volatiles are also produced from residual solvent during curing. Because aromatic polyimides are insoluble and infusible, a polyimide precursor consisting of polyamic acid (PAA) in a high boiling polar solvent such as NMP has been used to decrease the viscosity of polyimides. PAA is converted into polyimide through curing, and the volatilization of solvents and by-products creates voids in the polyimides [15–17].

In this study, there were no visible micro-sized voids in the polyimide adhesives for butt and single lap joints, as determined by a digital microscopy (data not shown) for fractured surface observations.[3] The polyimide adhesive joints were successfully fabricated using the layer-by-layer technique, drying process and autoclave curing.

After curing, fillets of adhesive at all edges of the specimens were carefully removed with a knife[4] and sandpaper and finely polished to measure the adhesive thickness. The adhesive thickness, h of the joints was measured using a digital microscope (Keyence, VHX-1000 and VH-Z100).

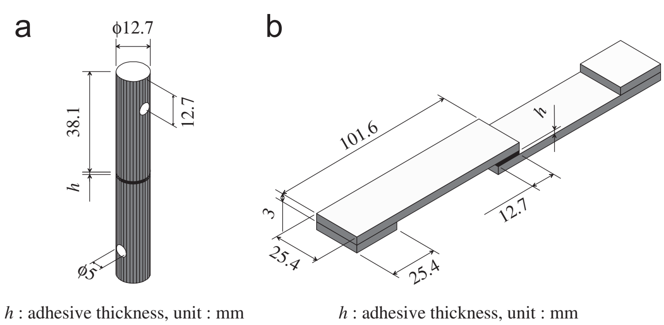

Fig. 1. Shapes and dimensions of the butt and single lap joints. (a) butt joint. (b) single lap joint.

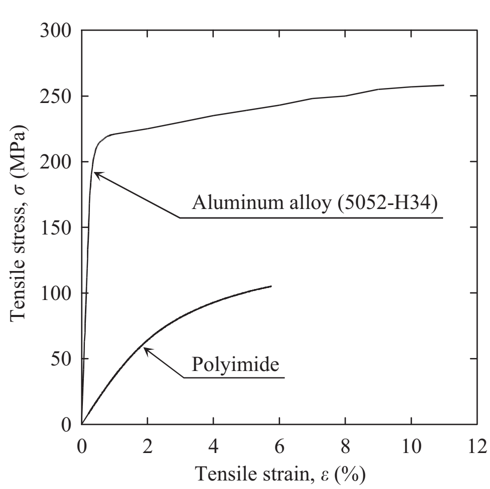

Fig. 2. Typical tensile stress-strain curves for the bulk polyimide and the aluminum alloy (5052-H34).

2.3. Static test

Static tensile and shear tests were conducted using a universal testing machine (Shimadzu, Autograph AG-series) with a load cell of 5 kN at a constant crosshead speed of 1.0 mm/min. All tests were conducted under the laboratory environment at room temperature (at 23 ± 3 °C and 50 ± 5 % relative humidity). The fracture morphology of these adhesive joints was examined using a scanning electron microscope (SEM, Topcon, SM-510) at an operating voltage of 15 kV.

3. Results and discussions

3.1. Effects of adhesive thickness on tensile and shear strength

For butt and single lap joints, the load applied to the specimen was almost linearly proportional to the displacement until failure.

[1] In the butt and single lap joints of thicker adhesive thickness, a small amount of the precursor solution was cast on bonding surface at room temperature, degassed in a vacuum oven at 90 ± 10 °C for 20 min to remove bubbles and then dried in an oven at 90 ± 10 °C for 4 h. This step was repeated until a solid material of appropriate amount was obtained. The layer-by-layer technique was applied.

[2] The crystalline structure of aluminum alloy (5052) changes at about 200 °C and the hardness of the aluminum alloy decreased. However, the tensile modulus of the alloy is similar to that in as-received state [38].

[3] There are no visible voids in the adhesive layer dried at 90 ± 10 °C for 12 hours. However, the visible voids were observed in the adhesive layer dried at 90 ± 10 °C for less (2 and 6 h) and more hours (24 h). Note that the residual solvent content in polyimide adhesive joints should be controlled to avoid the presence of voids.

[4] The fillets of adhesive at all edges of the specimens usually have some cracks or voids (probably due to drying process and external pressure for autoclave). Polyimide in these regions is not too rigid comparing with that in the adhesive layers.

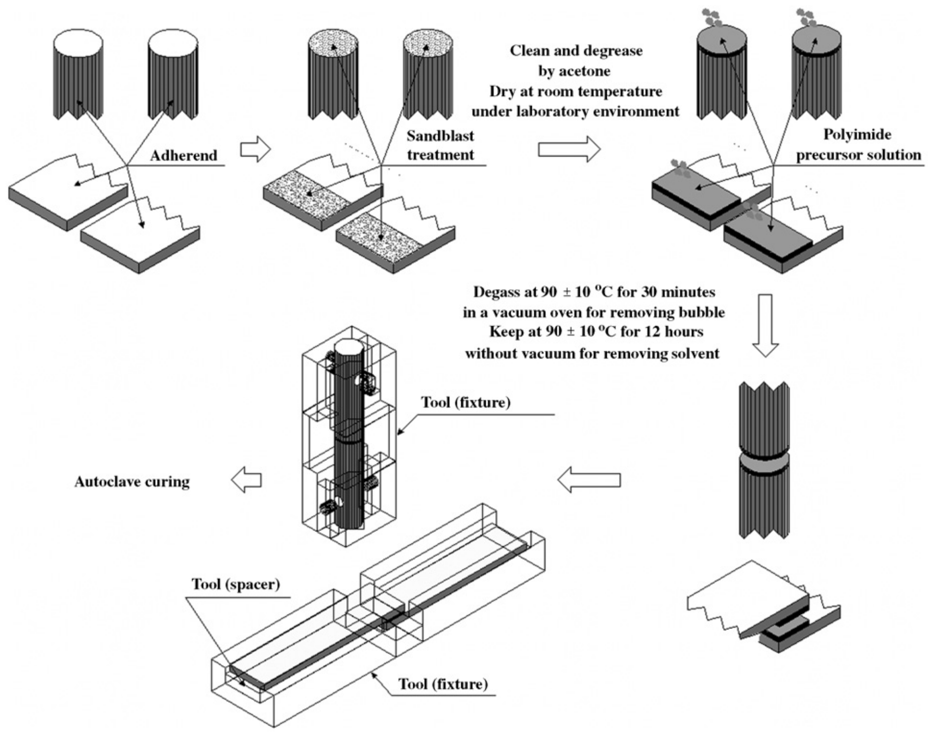

Fig. 3. Fabrication procedure of the butt and single lap joints.

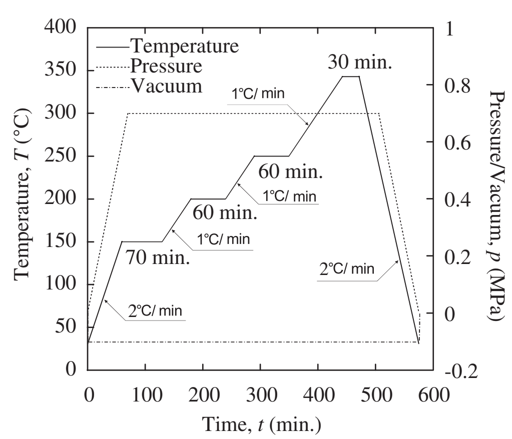

Fig. 4. Temperature, vacuum pressure and pressure profiles as a function of time.

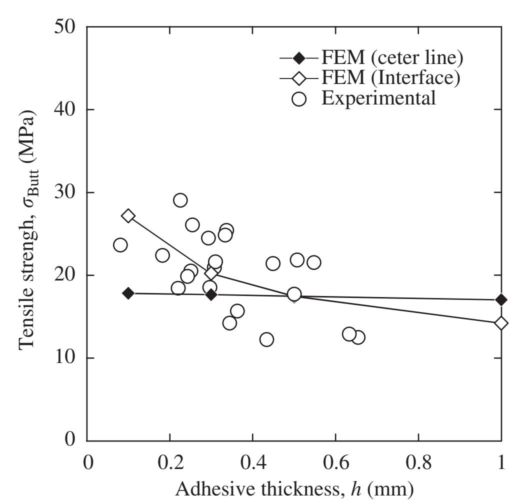

Fig. 5. Relation between the adhesive thickness and the tensile strength for butt joint.

Fig. 5 shows the relationship between tensile strength, σ_{Butt}($\sigma_{Butt}=P_{max}/A_{Butt}$, P_{max}: maximum load, A_{Butt}: adhesive bonded area) and adhesive thickness, h for butt joint. The figure confirms that the tensile strength of polyimide adhesive decreases with an increase in adhesive thickness. The measured adhesive thickness (h) and tensile strength (σ_{Butt}) are summarized in Table 1.

Fig. 6 shows the relationship between shear strength, τ_{Single}($\tau_{Single}=P_{max}/A_{Single}$, P_{max}: maximum load, A_{Single}: adhesive bonded area) and adhesive thickness, h for single lap joint. Shear strengths of the polyimide adhesive were almost constant regardless of adhesive thickness. The measured adhesive thickness (h) and shear strength (τ_{Single}) are summarized in Table 1.

A lot of scatter was observed in the tensile and shear strength of polyimide adhesive. The difference for the tensile strength of polyimide adhesive with similar adhesive thickness was tried to classify the fracture surfaces into the characteristic fracture patterns. In this study, however, the fracture morphological difference among the polyimide adhesive was not observed and it was difficult to classify the fracture surfaces of polyimide adhesive into the characteristic patterns.

The reasons of scatter for micro-sized voids (see section 2.2) and fracture patterns are therefore discounted. Instead, a stress state (including the stress concentration and/or the stress singularity) related to fracture mode was identified as the dominant reasons of scatter.

Fig. 7 shows the schematic view of fractured surfaces for butt and single lap joints.

The failures for butt and single lap joints were initiated at the interface between the adherend and the adhesive. Subsequently, these cracks propagated into the adhesives, the mixed mode of fracture (cohesive and interfacial failure) was observed. The fracture surfaces of these joints at the edge (interfacial failure regions), as also shown in Fig. 7, were examined using a SEM.

Table 1
Tensile and shear strength for butt and single lap joints with respect to adhesive thickness[a].

Adhesive thickness, $h_{(\mathrm{target})}$ (mm)		0.1	0.2	0.3	0.4	0.5	0.6	0.7	0.8	0.9	1.0
Butt joint											
Adhesive thickness, $h_{(\mathrm{measured})}$ (mm)			0.218 (0.025)	0.294 (0.033)	0.406 (0.061)	0.519 (0.026)	0.590 (0.060)				
Tensile strength, σ_{Butt} (MPa)			22.45 (4.71)	20.93 (3.88)	18.56 (4.05)	17.50 (4.46)	15.67 (5.10)				
Butt joint (FEM analysis)											
Estimated tensile strength $\sigma_{\mathrm{Butt}}^{\mathrm{FEM\ (normal\ stress)}}$ (MPa)	Center line	17.77		17.63		< 17.50 >					17.14
	Interface	27.42		20.28		< 17.50 >					14.20
Estimated tensile strength $\sigma_{\mathrm{Butt}}^{\mathrm{FEM\ (principal\ stress)}}$ (MPa)	Center line	17.77		17.63		< 17.50 >					17.14
	Interface	27.26		20.25		< 17.50 >					14.21
Estimated tensile strength $\sigma_{\mathrm{Butt}}^{\mathrm{FEM\ (von\ Mises\ stress)}}$ (MPa)	Center line	17.96		17.73		< 17.50 >					16.89
	Interface	26.87		20.18		< 17.50 >					14.26
Single lap joint											
Adhesive thickness, $h_{(\mathrm{measured})}$ (mm)		0.089 (0.066)	0.208 (0.026)	0.318 (0.025)	0.382 (0.027)	0.499 (0.021)	0.620 (0.019)	0.711 (0.021)		0.909 (0.027)	
Shear strength, τ_{Single} (MPa)		8.65 (0.90)	8.48 (0.99)	9.42 (0.97)	9.57 (0.87)	9.82 (0.58)	10.01 (0.83)	9.45 (1.44)		8.62 (1.50)	
Single lap joint (FEM analysis)											
Estimated shear strength $\tau_{\mathrm{Single}}^{\mathrm{FEM\ (normal\ stress)}}$ (MPa)	Center line	4.79		8.07		< 9.82 >					11.86
	Interface	9.24		9.86		< 9.82 >					9.17
Estimated shear strength $\tau_{\mathrm{Single}}^{\mathrm{FEM\ (shear\ stress)}}$ (MPa)	Center line	5.01		8.06		< 9.82 >					11.93
	Interface	9.03		9.86		< 9.82 >					9.17
Estimated shear strength $\tau_{\mathrm{Single}}^{\mathrm{FEM\ (principal\ stress)}}$ (MPa)	Center line	4.79		8.07		< 9.82 >					11.87
	Interface	9.19		9.86		< 9.82 >					9.17
Estimated shear strength $\tau_{\mathrm{Single}}^{\mathrm{FEM\ (von\ Mises\ stress)}}$ (MPa)	Center line	4.79		8.07		< 9.82 >					11.86
	Interface	9.09		9.86		< 9.82 >					9.17

( ) indicate standard deviations.

[a] The standard deviations of adhesive thickness were mainly caused by the difference among the specimens. The thickness differences of an individual specimen were 1/100 lower than those among the specimens.

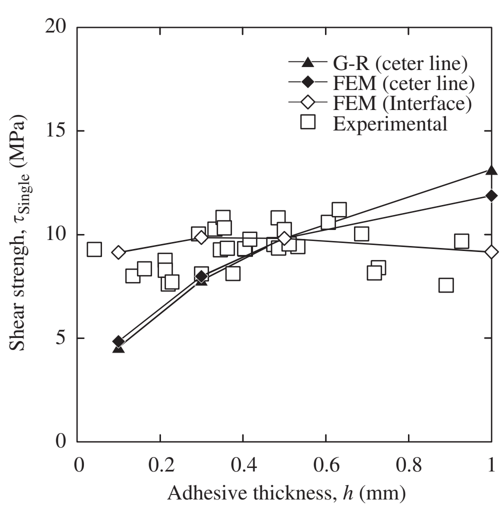

Fig. 6. Relation between the adhesive thickness and the shear strength for single lap joint.

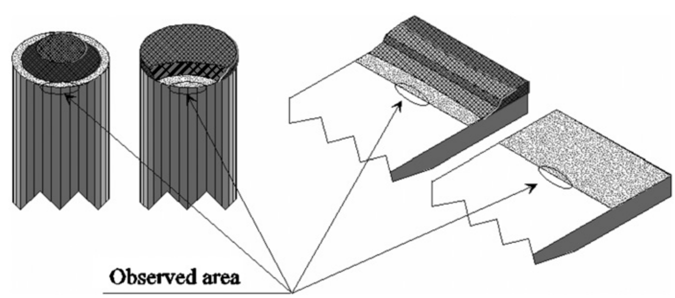

Fig. 7. Schematic view of fractured surfaces for butt and single lap joints.

Fig. 8 shows the SEM micrographs of sandblast treated adherend and interfacial fractured surfaces at the edge for butt and single lap joints.

Fracture surfaces of butt and single lap joints at the edge (interfacial failure regions) were similar to the surface of sandblast treated adherend. The fracture mode is strongly related to the joint strengths.

In this study, the sandblast treatment was applied to the adherends and interfacial failure occurred in butt and single lap joints. The fracture mode and the joint strengths are strongly depended on the adherend surface treatment. It is necessary to apply the sulfuric or chromic acid surface treatment for adherends in order to improve the interfacial bonded strength. In addition, the sulfuric or chromic acid surface treatment yields a relatively smooth surface as opposed to the sandblast treatment. This may lead to the more constant adhesive thickness.

3.2. FEM analysis

The effects of adhesive thickness on the joint strength were examined using the finite element method (FEM) analysis. Fig. 9 shows the typical FEM model for the butt and single lap joints

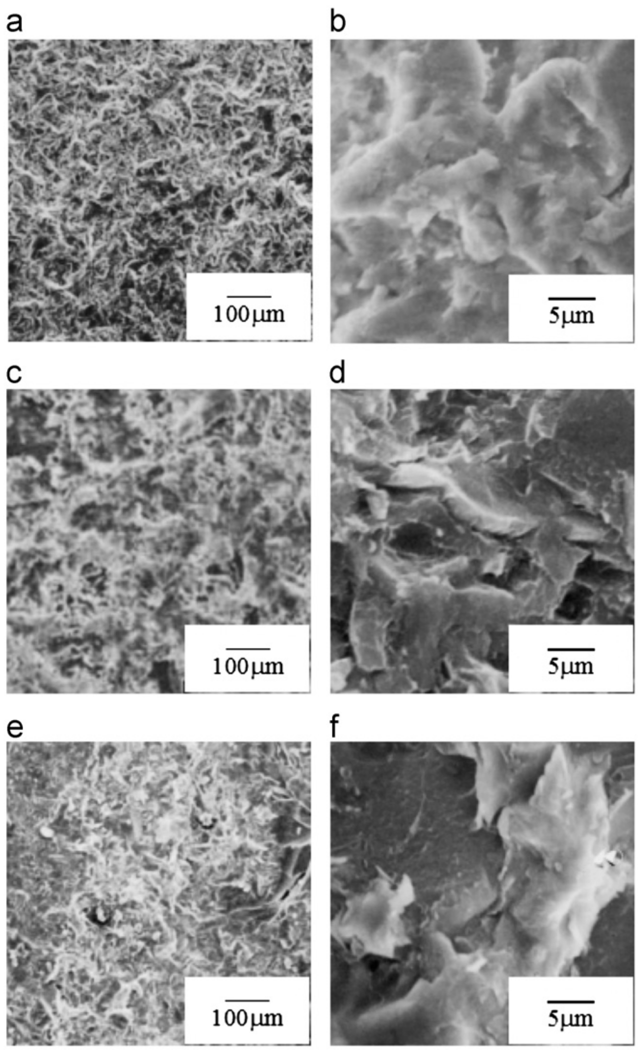

Fig. 8. SEM micrographs of sandblast treated adherend surface and interfacial fractured surfaces at the edge for butt and single lap joints. (a) sandblast at low magnification. (b) sandblast at high magnification. (c) butt joint at low magnification. (d) butt joint at high magnification. (e) single lap joint at low magnification. (f) single lap joint at high magnification.

(adhesive thickness, h=0.3 mm). 8-noded isoparametric quadrilateral elements in axisymmetric condition for butt joint and plane strain condition for single lap joint were used in these models.[5] Four different adhesive thickness (h=0.1, 0.3, 0.5 and 1.0 mm) were used in this calculation. The nodes/elements of butt and single lap joints were 4961/1600 (butt, h=0.1 mm), 6303/2040 (butt, h=0.3 mm), 6547/2120 (butt, h=0.5 mm), 7157/2320 (butt, h=1.0 mm), 13921/4500 (single lap, h=0.1 mm), 17925/5820 (single lap, h=0.3 mm), 18653/6060 (single lap, h=0.5 mm) and 20473/6660 (single lap, h=1.0 mm), respectively. Linear elastic analysis was performed on the butt and single lap joints with material properties of adherend and adhesive defined in Table 2 [36,37].[6] The

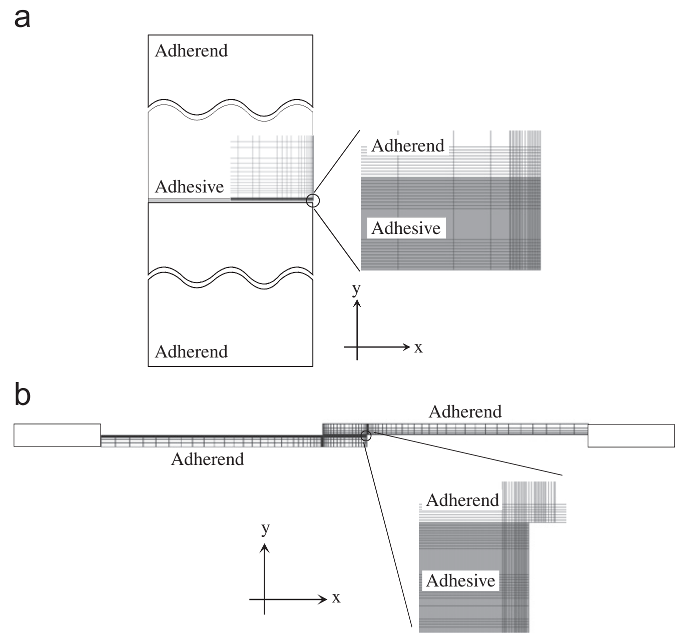

Fig. 9. Finite element method (FEM) model. (a) butt joint. (b) single lap joint.

Table 2
Material Properties of adherend and adhesive.

Adherend Young's modulus, E	69,600 MPa
Adherend Poisson's ratio, v	0.33
Adhesive Young's modulus, E_a	3770 MPa
Adherend Poisson's ratio, v_a	0.342

applied loads for butt and single lap joints are 2.217 kN (σ_{Butt}= 17.50 MPa) and 3.168 kN (τ_{Single}=9.82 MPa), respectively. These values are average tensile and shear strengths in adhesive thickness of 0.5 mm, as shown in Table 1.

Fig. 10 shows the normal stress, σ_y (peel stress), principal stress, σ_p and equivalent stress (von Mises stress), σ_{Mises} variations along the center line of adhesive layer and the interface between the adherend and the adhesive near the edges for butt joint and Fig. 11 shows the normal stress, σ_y (peel stress), shear stress, τ_{xy}, principal stress, σ_p and equivalent stress (von Mises stress), σ_{Mises} variations along the center line of adhesive layer and the interface between the adherend and the adhesive near the edges for single lap joint.[7]

In butt and single lap joints, the normal (σ_y), shear (τ_{xy}, only single lap joint), principal (σ_p) and equivalent (σ_{Mises}, von Mises) stress along the interface was higher than those along the center line for each adhesive thickness. That is, the stress (σ_y, τ_{xy} (only single lap joint), σ_p and σ_{Mises}) concentrated around the interface between the adherend and the adhesive due to the stress singularity.

For the butt joint as shown in Fig. 10, the σ_y, σ_p and σ_{Mises} along the center line near the edge were almost similar among the adhesive thickness. However, the difference of the σ_y, σ_p and σ_{Mises} along the interface by adhesive thickness was observed near

[5] In this study, fillets of adhesive at all edges of the specimens were removed. The stress singularity for butt (different materials in 90°/90° corner) and single lap (different materials in 90°/180° corner) joints was occurred. These results also observed in Dunders' composite parameter [39] and Bogy's stress singularity factor [40,41].

[6] The tensile stress–strain curves of the polyimide and aluminum alloy showed nonlinear behavior, as shown in Fig. 2. A little adherend plastic deformation during single lap joint test (did not get adherend plastic deformation during butt joint test) and the similar results in FEM analysis were observed. However, failure stress obtained from butt and single lap joints was quite low and plastic

(*footnote continued*)
deformation zones were small. Therefore, it was possible to apply the linear elastic analysis.

[7] The stress of each element was computed in Gauss point. Then, the stress of node was calculated in extrapolation manner. The stress of nodes obtained from the neighborhood elements was averaged.

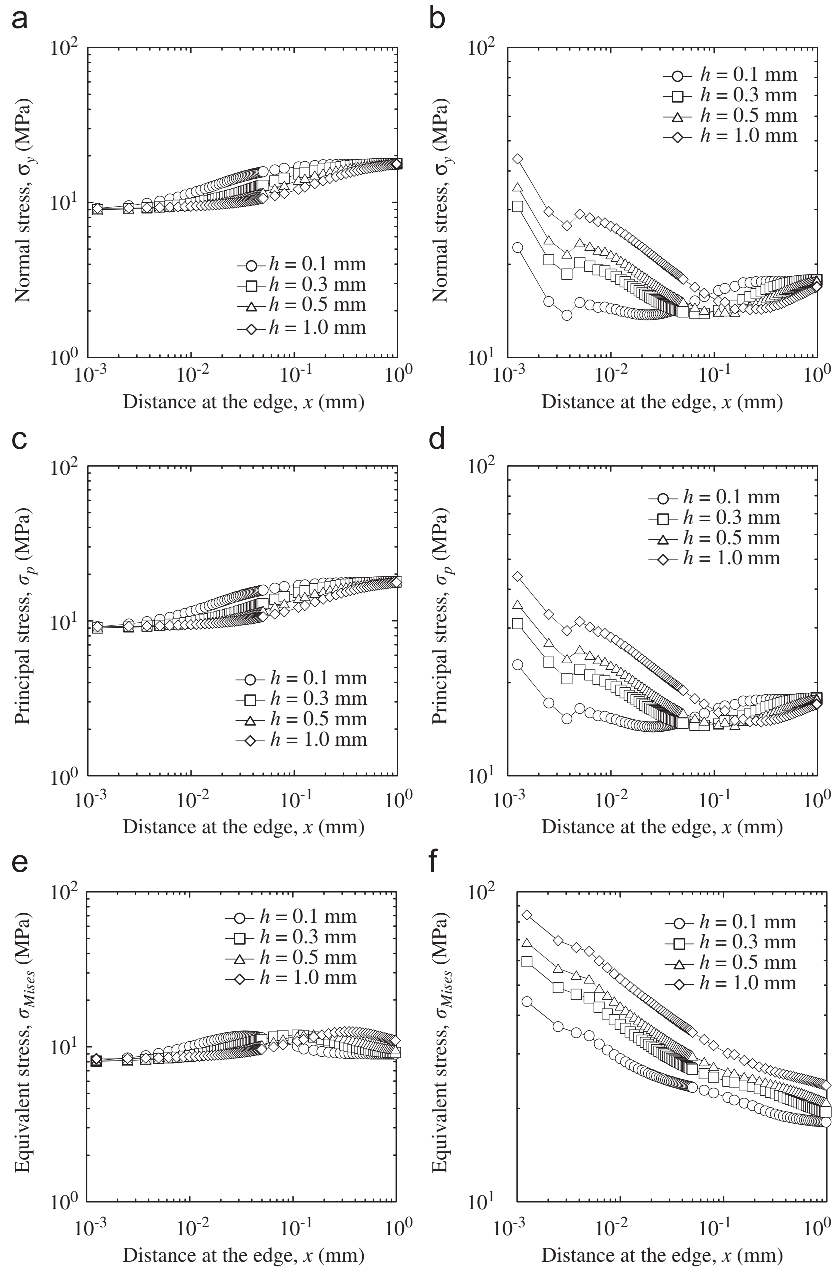

Fig. 10. Stress distributions along the center line of adhesive layer and the interface between the adherend and the adhesive near the edges for butt joint. (a) σ_y in center line. (b) σ_y in interface. (c) σ_p in center line. (d) σ_p in interface. (e) σ_{Mises} in center line. (f) σ_{Mises} in interface.

the edge. The σ_y, σ_p and σ_{Mises} along the interface near the edge increased with increasing adhesive thickness.

Although the shearing force (shear stress, τ_{xy}) is applied to the single lap joint, normal stress, σ_y (peel stress) in the adhesive layer at the edge must govern the final failure as well as crack initiation. The principal and equivalent (von Mises) stress distributions strongly depended on the normal stress distribution. For the single lap joint as shown in Fig. 11, the σ_y, τ_{xy}, σ_p and σ_{Mises} along the interface near the edge was almost similar among the adhesive thickness. However, the σ_y, τ_{xy}, σ_p and σ_{Mises} along the center line near the edge increased with decreasing adhesive thickness and similar result (effect of adhesive thickness on the stress distributions) was obtained from the normal (σ_y) and shear (τ_{xy}) stress in Goland–Reissner's analysis [42–46]. According to the normal, shear (only single lap joint), principal and equivalent (von Mises) stress distribution along the interface for this FEM analysis, the tensile strength of butt joint might decrease with increasing adhesive thickness and the shear strength of single lap joint might be almost constant among the adhesive thickness.

The effects of adhesive thickness on tensile and shear strength were predicted based on the normal, shear (only single lap joint), principal and equivalent (von Mises) stress distribution obtained from the FEM analysis. Fig. 12 shows the prediction procedures.

The stress distributions (σ_y, τ_{xy} (only single lap joint), σ_p and σ_{Mises}) along the center line of adhesive layer and the interface between the adherend and the adhesive for butt and single lap joints were calculated as shown in Figs. 10 and 11. In the center line, the horizontal axis was modified from "Distance at the edge, x" to "Effective distance at the edge, x/h" and the stress distributions along the center line were calculated so that the stress distributions near the edge for 0.1, 0.3 and 1.0 mm of adhesive thickness turned into the similar stress distributions for 0.5 mm of adhesive thickness. In the interface, the stress distributions along the interface were also calculated so that the stress

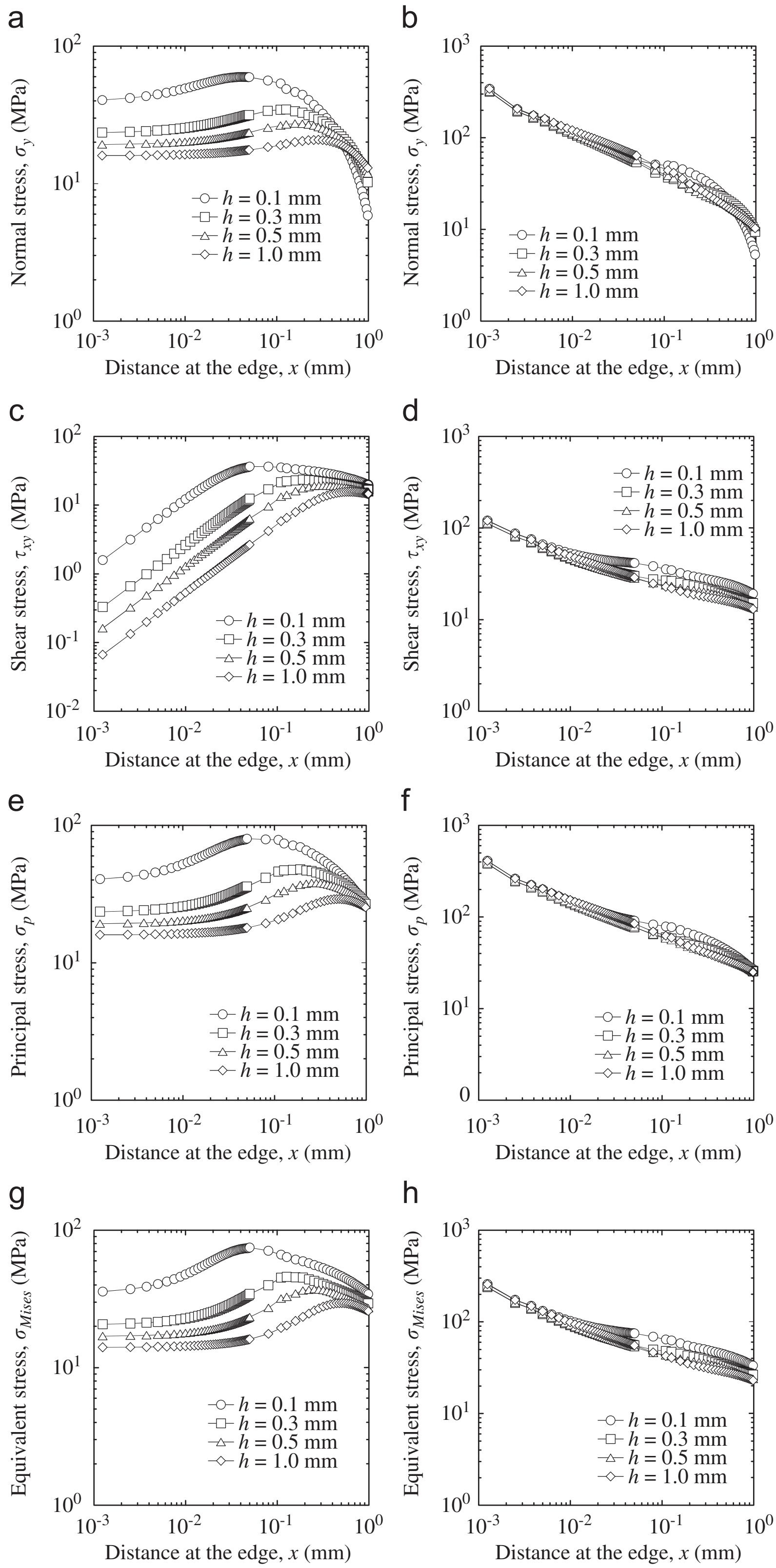

Fig. 11. Stress distributions along the center line of adhesive layer and the interface between the adherend and the adhesive near the edges for single lap joint. (a) σ_y in center line. (b) σ_y in interface. (c) τ_{xy} in center line. (d) τ_{xy} in interface. (e) σ_p in center line. (f) σ_p in interface. (g) σ_{Mises} in center line. (h) σ_{Mises} in interface.

distributions near the edge for 0.1, 0.3 and 1.0 mm of adhesive thickness turned into the similar stress distributions for 0.5 mm of adhesive thickness. The estimated applied load was obtained from the minimum error by solving numerically using a Newton–Raphson method. The estimated results of σ_y and σ_{Mises} variations along the center line of adhesive layer and the interface between the adherend and the adhesive near the edges for butt and single lap joints were also shown in Fig. 12.

The effects of adhesive thickness on tensile and shear strength were predicted based on the above procedure. The predicted

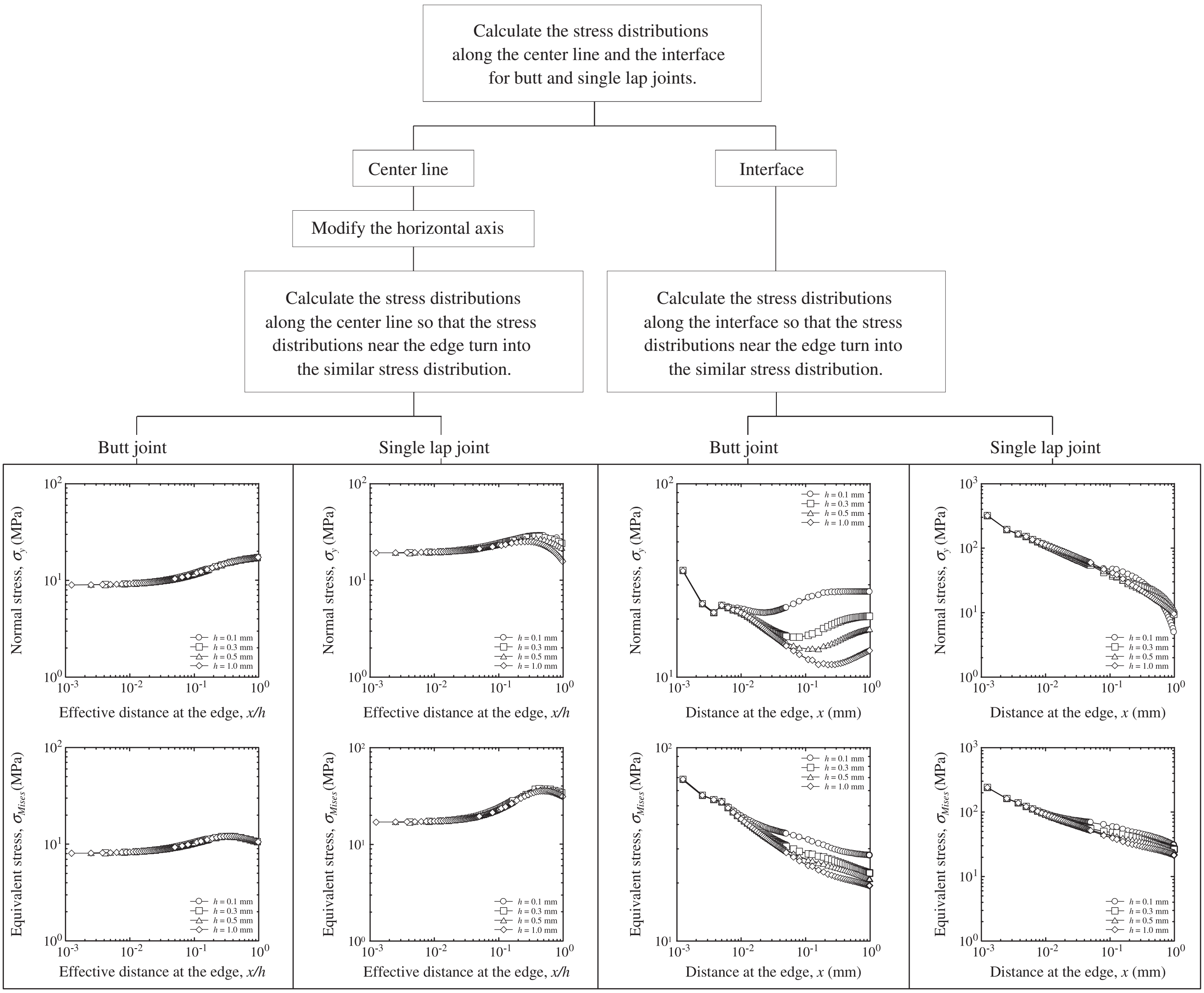

Fig. 12. Prediction procedures for tensile and shear strength for butt and single lap joints.

results were shown in Figs. 5 and 6,[8] and summarized in Table 1. For the single lap joint, the analytical results using the normal (σ_y) and shear (τ_{xy}) stress in Goland–Reissner's analysis (G–R (center line)) were also shown in Fig. 6.[9] The predicted results for the butt and single lap joints were almost similar among the each stress distributions (σ_y, τ_{xy} (only single lap joint), σ_p and σ_{Mises}). Using the stress distributions (σ_y, τ_{xy} (only single lap joint), σ_p and σ_{Mises}) along the center line, the tensile strength was not affected by adhesive thickness and the shear strength increased with increasing adhesive thickness. However, using the stress distributions (σ_y, τ_{xy} (only single lap joint), σ_p and σ_{Mises}) along the interface between the adherend and the adhesive, the tensile strength decreased with increasing adhesive thickness and the shear strength was not affected by adhesive thickness. The analytical results using the stress distributions (σ_y, τ_{xy} (only single lap joint), σ_p and σ_{Mises}) along the interface for both joints are good agree with the experimental results. The effects of adhesive thickness on tensile and shear strength depended on the failure mode and could be explained based on the surface observation and the stress distributions obtained from the FEM analysis.[10]

[8] The predicted results showed in Figs. 5 and 6 were averaged results obtained from the σ_y, τ_{xy} (only single lap joint), σ_p and σ_{Mises}.

[9] The Goland–Reissner's analytical result showed in Fig. 6 was also averaged result obtained from the σ_y and τ_{xy}.

[10] In the butt joint, the stress in the center line was confirmed the FEM analytical results with the applied stress and the stress in the interface was the following equation;

$$\sigma_y = \frac{K_y}{x^{\lambda}}$$

where K_y and λ are intensity of stress singularity and stress singularity factor, respectively. The stress singularity factor, λ was calculated using the Bogy's analysis [40,41] (different materials in 90°/90° corner) and the λ was 0.260. The stress singularity factors, λ obtained from the FEM analysis were almost similar among the adhesive thickness (λ=0.265). In addition, the intensities of stress singularity, K_y obtained from the predicted results were also almost similar among the adhesive thickness (K_y=5.48).

In the single lap joint, the stress in the center line was confirmed the FEM analytical results with the Goland–Reissner's analytical results. The stress in the interface was also confirmed the intensity of stress singularity and stress singularity factor. The stress singularity factor, λ was calculated using the Bogy's analysis (different materials in 90°/180° corner), although the loading direction between the FEM and Bogy's analysis was slightly different, and the λ was 0.335. The stress singularity factors, λ obtained from the FEM analysis were almost similar among the adhesive thickness (λ=0.524). In addition, the intensities of

4. Conclusions

The conventional butt and single lap joints using the high temperature polyimide adhesive were fabricated and the effects of adhesive thickness on static joint strength of polyimide adhesive were investigated for butt and single lap joints. From the experiments and FEM stress analyses, the following conclusions were obtained.

(1) There are no visible micro-sized voids in the polyimide adhesives for butt and single lap joints. The polyimide adhesive joints are successfully fabricated using the layer-by-layer technique, drying process and autoclave curing.
(2) Tensile strength for butt joint decreases with increasing adhesive thickness and shear strength for single lap joint is almost constant regardless of adhesive thickness, although a lot of scatter is observed in the tensile and shear strength of polyimide adhesive.
(3) The fabricated joints failed in an interfacial manner and the effects of adhesive thickness on tensile and shear strength could be explained based on the failure mode and the stress distributions obtained from the FEM analysis.

References

[1] Cole GS, Sherman AM. Lightweight materials for automotive applications. Mater Charact 1995;35(1):3–9.
[2] Immarigeon JP, Holt RT, Koul AK, Zhao L, Wallace W, Beddoes JC. Lightweight materials for aircraft applications. Mater Charact 1995;35(1):41–67.
[3] Matsuzaki R, Shibata M, Todoroki A. Reinforcing an aluminum/GFRP co-cured single lap joint using inter-adherend fiber. Compos Part A-Appl S 2008;39(5):786–95.
[4] Rhee KY, Lee SG, Choi NS, Park SJ. Treatment of CFRP by IAR method and its effect on the fracture behavior of adhesive bonded CFRP/aluminum composites. Mat Sci Eng A-struct 2003;357(1-2):270–6.
[5] Hornung M, Hajj M. Structural bonding for lightweight construction. Mater Sci Forum 2009;618-619:49–56.
[6] Tai RCL, Szklarskasmialowska Z. Effect of fillers on the degradation of automotive epoxy adhesives in aqueous solutions Part I Absorption of water by different fillers-incorporated automotive epoxy adhesives. J Mater Sci 1993;28(22):6199–204.
[7] Kahraman R, Al-Harthi M. Moisture diffusion into aluminum powder-filled epoxy adhesive in sodium chloride solutions. Int J Adhes Adhes 2005;25(4): 337–41.
[8] da Silva LFM, Öchsner A, Adams RD, editors. Handbook of Adhesion Technology, vol. 1. Springer, Verlag; 2011.
[9] May CA. Epoxy resins. In: Reinhart TJ, Dostal CA, Woods MS, Frissell HJ, Ronke AW, editors. Engineered materials handbook, vol. 1. Ohio: Composites, ASM International; 1988. p. 66–77.
[10] Behm DT, Gannon J. Epoxies. In: Brinson HF, Dostal CA, Woods MS, Ronke AW, Henry SD, Daquila JL, editors. Engineered materials handbook, vol. 3. Ohio: Ahesives and sealants, ASM International; 1990. p. 94–102.
[11] Juska TD, Puckett PM. Matrix resins and fiber/matrix adhesion. In: Mallick PK, editor. Composites engineering handbook. New York: Marcel Dekker Inc.; 1997. p. 101–65.
[12] Landis AL, Lau KSY. High-performance polyimides and related thermoset polymer: Past and present development, and future research directions. In: Goodman SH, editor. Handbook of thermoset plastics. 2nd ed. New Jersey: Noyes Publications; 1998. p. 302–467.
[13] Ghosh MK, Mittal KL. Polyimides: Fundamentals and applications. New York: Marcel Dekker Inc.; 1996.
[14] Rossi RD. Polyimides. In: Brinson HF, Dostal CA, Woods MS, Ronke AW, Henry SD, Daquila JL, editors. Engineered materials handbook, vol. 3. Ohio: Ahesives and sealants, ASM International; 1990. p. 151–62.
[15] da Silva LFM, Adams RD, Gibbs M. Manufacture of adhesive joints and bulk specimens with high-temperature adhesives. Int J Adhes Adhes 2004;24(1): 69–83.
[16] Saunders RA, Lekakou C, Bader MG. Compression in the processing of polymer composites 1. A mechanical and microstructural study for different glass fabrics and resins. Compos Sci Technol 1999;59(7):933–83.

(*footnote continued*)
stress singularity, K_y obtained from the predicted results were also almost similar among the adhesive thickness (K_y=9.12).

[17] Thomason JL. The interface region in glass-fiber-reinforced epoxy-resin composites: Part 1. Sample preparation, void content and interfacial strength. Composites 1995;26(7):467–75.
[18] Bowles KJ, Frimpong S. Void effects on the interlaminar shear-strength of unidirectional graphite-fiber-reinforced composites. J Compos Mater 1992;26(10):1487–509.
[19] Farouk A, Kwon TH. Effect of processing parameters on compression molded PMR-15/C3K composites. Polym Compos 1990;11(6):379–86.
[20] ASTM D2094-00. Standard practice for preparation of bar and rod specimens for adhesion tests. ASTM annual book of standards, vol. 15.06, West Conshohocken, PA; 2009.
[21] ASTM D2095-96. Standard test method for tensile strength of adhesives by means of bar and rod specimens. ASTM annual book of standards, vol. 15.06, West Conshohocken, PA; 2009.
[22] Osswald TA, Rietveld J. Measuring constitutive properties. In: Brinson HF, Dostal CA, Woods MS, Ronke AW, Henry SD, Daquila JL, editors. Engineered materials handbook, vol. 3. Ohio: Ahesives and sealants, ASM International; 1990. p. 315–24.
[23] ASTM D1002-05. Standard test method for apparent shear strength of single-lap-joint adhesively bonded metal specimens by tension loading (metal-to-metal). ASTM annual book of standards, vol. 15.06, West Conshohocken, PA; 2009.
[24] Grant LDR, Adams RD, da Silva LFM. Experimental and numerical analysis of single-lap joints for automotive industry. Int J Adhes Adhes 2009;29(4):405–13.
[25] da Silva LFM, Carbas RJC, Critchlow GW, Figueiredo MAV, Brown K. Effect of material, geometry, surface treatment and environment on the shear strength of single lap joints. Int J Adhes Adhes 2009;29(6):621–32.
[26] Adams RD. Failure strength tests and their limitations. In: Brinson HF, Dostal CA, Woods MS, Ronke AW, Henry SD, Daquila JL, editors. Engineered materials handbook, vol. 3. Ohio: Ahesives and sealants, ASM International; 1990. p. 325–34.
[27] Sperandio C, Bardon J, Laachachi A, Aubriet H, Ruch D. Influence of plasma surface treatment on bond strength behaviour of an adhesively bonded aluminium-epoxy system. Int J Adhes Adhes 2010;30(8):720–8.
[28] Higgins A. Adhesive bonding of aircraft structures. Int J Adhes Adhes 2000;20(5):367–76.
[29] Fessel G, Broughton JG, Fellows NA, Durodola JF. Evaluation of different lap-shear joint geometries for automotive applications. Int J Adhes Adhes 2007;27(7):574–83.
[30] da Silva LFM, Rodrigues TNSS, Figueiredo MAV, de Moura MFSF, Chousal JAG. Effect of adhesive type and thickness on the lap shear strength. J Adhesion 2006;82(11):1091–115.
[31] da Silva LFM, Critchlow GW, Figueiredo MAV. Parametric study of adhesively bonded single-lap joints by the Taguchi method. J Adhes Sci Technol 2008;22(13):1477–94.
[32] Tankut N. The effect of adhesive type and bond line thickness on the strength of mortise and tenon joints. Int J Adhes Adhes 2007;27(6):493–8.
[33] Mall S, Ramamurthy G. Effect of bond thickness on fracture and fatigue strength of adhesively bonded composites joints. Int J Adhes Adhes 1989;9(1):33–7.
[34] Azari S, Papini M, Spelt JK. Effect of adhesive thickness on fatigue and fracture of toughened epoxy joints—Part I: Experiments. Eng Fract Mech 2011;78(1):153–62.
[35] Park JH, Choi JH, Kweon JH. Evaluating the strengths of thick aluminum-to-aluminum joints with different adhesive lengths and thicknesses. Compos Struct 2010;92(9):2226–35.
[36] Naito K, Yang JM, Kagawa Y. The effect of nanoparticle inclusion on the tensile and mode I fracture properties of polyimides. Mat Sci Eng A-Struct 2011;530:357–66.
[37] Department of Defense Handbook. Metallic materials and elements for aerospace vehicle structures in MIL-HDBK-5J, Philadelphia, PA; 2003.
[38] Tsai TL, Sun PL, Kao PW, Chang CP. Microstructure and tensile properties of a commercial 5052 aluminum alloy processed by equal channel angular extrusion. Mat Sci Eng A-Struct 2003;342(1–2):144–51.
[39] Dunders J. Effect of elastic constants on stress in a composite under plane Deformation. J Compos Mater 1967;1(3):310–22.
[40] Bogy DB. Edge-bonded dissimilar orthogonal elastic wedges under normal and shear loading. J Appl Mech 1968;35(3):460–6.
[41] Bogy DB. On the problem of edge-bonded elastic quarter-planes loaded at the boundary. Int J Solids Struct 1970;6(9):1287–313.
[42] Goland M, Reissner E. The stresses in cemented joints. J Appl Mech 1944;66:A17–27.
[43] Wu ZJ, Romeijn A, Wardenier J. Stress expressions of single-lap adhesive joints of dissimilar adherends. Compos Struct 1997;38(1–4):273–80.
[44] Reis PNB, Antunes FJV, Ferreira JAM. Influence of superposition length on mechanical resistance of single-lap adhesive joints. Compos Struct 2005;67(1):125–33.
[45] da Silva LFM, das Neves PJC, Adams RD, Spelt JK. Analytical models of adhesively bonded joints-part I: Literature survey. Int J Adhes Adhes 2009;29(3):319–30.
[46] da Silva LFM, das Neves PJC, Adams RD, Wang A, Spelt JK. Analytical models of adhesively bonded joints-part II: Comparative study. Int J Adhes Adhes 2009;29(3):331–41.